Temperature dependence of the dielectric function of germanium

L. Viña, S. Logothetidis,* and M. Cardona
Max-Planck-Institut für Festkörperforschung, Heisenbergstrasse 1, 7000 Stuttgart 80, Federal Republic of Germany
(Received 16 April 1984)

Ellipsometric measurements of the dielectric constant of undoped Ge were performed between 1.25 and 5.6 eV in the temperature range of 100 to 850 K. The dependence of the E_1, $E_1+\Delta_1$, E_0', and E_2 critical energies on temperature was obtained. It can be represented either with Varshni's empirical formula or with an expression proportional to the Bose-Einstein statistical factor of an average phonon. Broadening parameters, amplitudes, and phase angles for the corresponding critical points were also obtained. A decrease of the excitonic interaction with increasing temperature was found. The results are discussed in the light of recent calculations of the effect of temperature on the band structure of Ge containing Debye-Waller and self-energy contributions.

I. INTRODUCTION

Germanium is, together with silicon, the most thoroughly studied semiconductor. A wide variety of experiments have given detailed information about its band structure. Among them optical experiments play a predominant role. Transmission of light through thin epitaxial films,[1–4] thinly ground samples,[5–14] and cleaved samples[15] was probably the first optical technique used. These experiments were in some cases performed as a function of an external parameter such as a magnetic field,[16–18] an electric field,[19,20] crossed electric and magnetic fields,[21] pressure,[6,8,22] or temperature.[23] Reflectivity measurements were also performed in the early years.[24–31] The reflectivity spectrum was sometimes measured over a sufficient energy range to permit Kramers-Kronig analysis of the data, so as to obtain the optical constants.[2,32–34] Reflectance modulation techniques have more recently provided invaluable information about structure in the optical spectra of Ge and many other semiconductors. Since the pioneering work of Seraphin[35,36] electroreflectance has become one of the most useful forms of band-structure spectroscopy,[37–56] together with piezoreflectance,[57–62] stress-modulated transmission,[60,63] piezoelectroreflectance,[64] magnetoelectroreflectance,[65,66] magnetopiezoreflectance,[67,68] thermoreflectance,[56,69] and wavelength modulation.[70–72]

In addition to Kramers-Kronig analysis, the refractive index of Ge has been obtained with interferometry,[1,7] the prism method (in the region of transparency only),[7,73,74] reflectance measurements at several angles of incidence,[29] pseudo-Brewster-angle,[75–77] and ellipsometry.[78–87]

In some of these works the temperature dependence of the optical constants or structures in the optical spectra have also been studied between liquid-helium and room temperature (RT),[10,12,13,20,31,60,71] at 30 K and RT,[44,47,49,79] liquid-N_2 and RT,[7,9,11,25,34,35,55,62,69,72] liquid-N_2 temperature and 500 K,[23] RT and 600 K,[73] and up to temperatures close to the melting point.[27,74,85] A detailed examination of the optical data available for Ge until 1967 was performed in Ref. 88 and a comparative study of the various values of the refractive index found in the literature was presented in Ref. 87.

Temperature-dependence studies of the optical constants are important from the theoretical and practical point of view: Due to the fact that the T dependence of structure in optical constants seems to be directly related to the T dependence of the band states involved in the process, these studies can be used to check band-structure calculations. From the applied science standpoint accurate knowledge of the changes of the refractive index with temperature is important among other things for designing solar energy converters and for understanding the laser-annealing process.[89,90]

The electronic structure of Ge has also been profusely studied theoretically. Many band-structure calculations with different approaches, some microscopic and some semiempirical, are available in the literature.[91–101] Theoretical work on the temperature dependence of the band structure is not so abundant. Two mechanisms are responsible for the temperature dependence of energy bands at constant pressure:[102] thermal expansion and renormalization of band energies by electron-phonon interactions. The first term can be calculated by combining the volume dependence of band energies with measured values of the thermal-expansion coefficient. Two types of electron-phonon interactions have been distinguished, Debye-Waller terms[103] and "self-energy" terms,[104,105] due to the first-order electron-phonon interaction. Calculations have focused only on the fundamental gap of semiconductors. In some work,[60,106,107] reasonable agreement with experiment has been obtained considering only the Debye-Waller terms. However, it has been shown that both terms should be included,[108,109] as was done recently in the case of Si and Ge.[110,111] An alternative approach found in the literature is to study the effects of electrons on phonons instead of the opposite.[112]

In spite of the large amount of experimental information available for the optical constants of Ge and other semiconductors, reliable data on the temperature dependence of these constants are limited to the region of transparency and the lowest absorption edge. Ellipsometric measurements at temperatures between 10 and 1000 K have been recently presented for Si.[113] In this paper we

report measurements of the optical constants of intrinsic Ge in the energy range from the near-infrared (1.25 eV) to the near-ultraviolet (5.6 eV) as a function of temperature from 100 to 850 K. The measurements were performed with an automatic rotating-analyzer ellipsometer. In addition to the real and imaginary parts of the function, our data yield accurate numbers for the shift and broadening of the higher interband transitions (labeled E_1, $E_1+\Delta_1$, E_0', and E_2) with temperature.

The first interpretation of Ge optical structure above the lowest direct edge in terms of direct interband transitions was given by Phillips,[114] the E_1 and $E_1+\Delta_1$ edges result from transitions in the Λ directions of the Brillouin zone (BZ) $\{111\}$, the E_0' edge, which also contains fine structure due to spin-orbit (SO) splitting,[51] has been assigned to different regions in the BZ: transitions between the $\Gamma_{25'}$ valence band and Γ_{15} conduction band, coincidence of a three-dimensional[30] (3D) minimum critical point (CP) at Γ with a 3D saddle point in the Δ direction of the BZ,[97,115] or a large region centered at $(2\pi/a)\times(0.33, 0.24, 0.14)$.[99] All these points are close in energy and $\vec{k}$ space to the $\Gamma_{25'}\rightarrow\Gamma_{15}$ gap.

The next structure E_2 has been alternatively attributed to an accidental coincidence of an M_1 saddle point at X and an M_2 saddle point in the Σ direction,[93] to a small region centered at $(2\pi/a)(0.77, 0.29, 0.16)$,[99] and more recently it is believed to originate mainly from a region in the Γ-X-U-L plane near $(2\pi/a)$ $(\frac{3}{4}, \frac{1}{4}, \frac{1}{4})$.[97,115] An onset of a new structure corresponding to transitions between $\Lambda_{4,5}$ and Λ_6 (E_1') is also seen at 5.5 eV.

The CP parameters amplitude A, energy threshold E, broadening Γ, and phase ϕ are obtained through analysis of numerical second-derivative spectra of the complex dielectric constant with respect to the photon energy, $d^2\epsilon/d\omega^2$. Two-dimensional (2D) critical points, allowing for excitonic effects in the form of a phase factor which mixes the real and imaginary parts of ϵ,[116] were used to fit the structures in the spectra. A mixture of a 3D M_0 with an M_1 CP was used for the E_0' and $E_0'+\Delta_0$ structures at low temperatures. The main effect of increasing the temperature is to broaden the CP and shift it to lower energies. We have fitted the CP energies to Varshni's empirical expression,[117] but we have found that the data can be fitted equally well to an expression proportional to the mean occupancy of an average phonon (see Fig. 6). This procedure also gives a reasonable fit to the broadening parameter of these structures.

In the following section, a description of the experimental details is first given. The results are presented in Sec. III and discussed in Sec. IV.

II. EXPERIMENTAL

The measurements were taken on a 500-μm-thick (110) pure-Ge sample (resistivity 40 Ω cm) in the temperature range from 100 to 850 K. The surfaces to be measured were mechanically lapped and polished with 0.75-μm grit Al_2O_3 powder. An etch-polish with Syton (Syton W30, Brenntag AG, 4330 Mülheim/Ruhr 12, Federal Republic of Germany) followed. They were finally polished with a bromine-methanol solution.[118] Dielectric function spectra $\epsilon(\omega)=\epsilon_1(\omega)+i\epsilon_2(\omega)$ were measured with an automatic rotating-analyzer ellipsometer.[119] The light from a lamp, after being dispersed by a $\frac{3}{4}$-m Spex monochromator, is linearly polarized with a Rochon-quartz prism. The linear-polarized light becomes generally elliptically polarized after reflection on the sample. The reflected light is modulated by means of a rotating analyzer (Rochon prism) and detected by a photomultiplier. The output of the photomultiplier is digitized and the digital signal analyzed with the aid of a model 9845B HP computer. Mirror optics is used for collimating and focusing the light. The spectra can be stored for later processing of data.

Two different light sources were used for the measurements: a tungsten quartz-iodine lamp (Osram Halogen-Bellaphot 64625, 12 V,100 W) for photon energies below 2.3 eV and a 75-W short-arc Xe lamp for the energy range from 1.8 to 5.6 eV. A 1200-line/mm Bausch and Lomb grating blazed at 1 μm and an EMI 9684B photomultiplier with S1 response cooled to -180 °C, were employed in combination with the quartz-iodine lamp and a 2400-line/mm Jobin-Yvon holographic grating together with an EMI 9558QB photomultiplier (S20 response) with the Xe lamp.

The sample, sealed in a stainless-steel holder with a commercial cement,[120] was mounted and optically aligned with an He-Ne laser in a windowless cell in flowing dry N_2 and was etched following the prescription of Ref. 118 to remove the distorted layer produced by mechanical polishing; real-time ellipsometric measurements at the energy of the E_2 peak were taken simultaneously. The treatment was repeated until no more changes took place and the highest value of ϵ_2 at E_2 was obtained.[118] A spectrum was measured immediately after etching. The sample was then again rinsed with methanol and placed in a cold-finger cryostat within minutes of the completion of the etch so as to minimize oxide formation. The measuring chamber was initially outgassed by heating to a temperature of $\sim$200 °C and pressure of 10^{-6} Torr for several hours. During all the process of measurement the vacuum was of the order of 3×10^{-8} Torr or better (a Ti ion-getter pump was used); this is necessary to avoid condensation of ice and oil films at low temperatures, which occurs if the pressure is worse than 10^{-7} Torr.

The cryostat was mounted on the ellipsometer and aligned with the He-Ne laser. Although we have used high-quality stress-free fused quartz windows,[121] a small systematic error is present in our measurements because of residual changes in the polarization of the light due to the windows. These were slightly misaligned with their normal nearly parallel to the light beam. By comparison of data taken on an Si sample covered with natural oxide with and without the windows in the measuring chamber, we conclude that the changes in the ellipsometric angles ψ and Δ introduced by the windows are at worst $\delta(\psi)<0.3°$, $\delta(\Delta)<0.7°$ (in the uv spectral region). This limits the accuracy of the ϵ data to $\pm5\%$. However, this does not modify the details of the structure present in the spectra. The sample temperature can be varied continuously by means of a resistance furnace mounted inside a copper sample holder. The sample temperature was determined

with a Chromel-Alumel thermocouple in contact with the back of the sample. Temperature stability was typically ± 1 K. The temperature range was limited by the cryostat construction. The procedure used to obtain drift stabilization and photomultiplier linearization[85] can also be used to correct the data for thermal light emission from the sample which appears as a dark current. All the spectra were taken at an angle of incidence of 67.5° with a mesh of 10 meV. The optical activity of the quartz was taken into account[122] and a calibration[122] was made at each temperature to correct for possible changes of the sample position due to the thermal expansion of the sample holder.

III. RESULTS

Using the measured ellipsometric angles (ψ,Δ) corrected pseudodielectric functions were calculated from the complex reflectance ratios. After the transfer of the sample to the cryostat and the process of outgassing, an oxide layer is still present. We estimate the thickness of this film to be 11 ± 2 Å by fitting room-temperature data obtained from the sample in the cryostat to the data measured immediately after etching in the windowless cell. A three-phase model[123] (air—GeO_2—bulk Ge) was used for the treatment of the data. It was assumed that the overlayer was GeO_2 with an index of refraction taken from the literature[124] and supposed to be independent of T.[83] The equations were solved to obtain $\epsilon(\omega)$ using the two-dimensional Newton's method.[125] The fact that fitting to the previous data before and after the heating cycle gave a change in the thickness ≤ 2 Å, allowed us to use the same oxide thickness for all temperatures.

The real and imaginary parts of the corrected pseudodielectric constant (ϵ) for four selected temperatures are shown in Figs. 1 and 2, respectively. Although the signal-to-noise ratio for the S1 was worse than for the S20 photomultiplier, the data from both sets of measurements (with S1 and S20) agree within 3% in the overlap region. In these figures we show data collected with both multipliers and matched smoothly in the region of overlap. The four main structures (E_1, $E_1+\Delta_1$, E_0', and E_2) shift to lower energies and broaden with increasing temperature. The peaks in ϵ_2 corresponding to the E_1 and $E_1+\Delta_1$ CP merge into a broad one. In these figures data taken from the literature at room temperature (○), 500 K (●), and 825 K (▲) are also shown. The sample orientation was [111] in the RT measurement. For the high-temperature ones it was not given. In view of the fact that different surface orientations are known to affect ϵ differently due to oxidation and chemical treatment,[118] the agreement is found to be excellent.

In order to enhance the structure present in the spectra and to obtain the CP parameters, we calculate numerically the second-derivative spectra, $d^2\epsilon/d\omega^2$, of the complex dielectric function from our ellipsometric data. Tabulated coefficients taken from the literature[126] were used to compute the derivatives: an appropriate level of smoothing was also allowed in order to suppress the noise in the derivative spectra without distorting the line shape. Another approach to investigate CP is to make a Fourier analysis of the rough data,[127] this method gives very precisely CP parameters without using numerical derivative procedures. It should be desirable to use it for our spectra and we plan to do it in future work. In Fig. 3 we show the experimental $d^2\epsilon_1/d\omega^2$ and $d^2\epsilon_2/d\omega^2$ of the E_1 and $E_1+\Delta_1$ transitions at 100 K. The derivative spectra were fitted to one-electron CP line shapes. A least-squares procedure was used for the fit, with both the real and the imaginary parts of $d^2\epsilon/d\omega^2$ fitted simultaneously. Excitonic effects were also taken into account in a conventional manner by allowing a mixture of two CP's.[116,128,129] Two different fits are presented in Fig. 3. The solid lines corre-

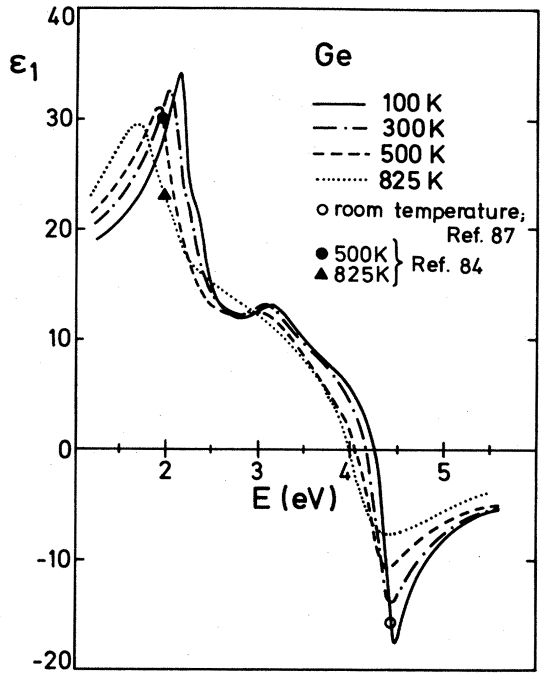

FIG. 1. Real part (ϵ_1) of the pseudodielectric function of Ge at 100 K (——), 300 K (—·—·—·), 500 K (— — —), and 825 K (·····). Single values obtained from the literature are room temperature, Ref. 87, (○), and 50 and 825 K (● and ▲, respectively) from Ref. 84.

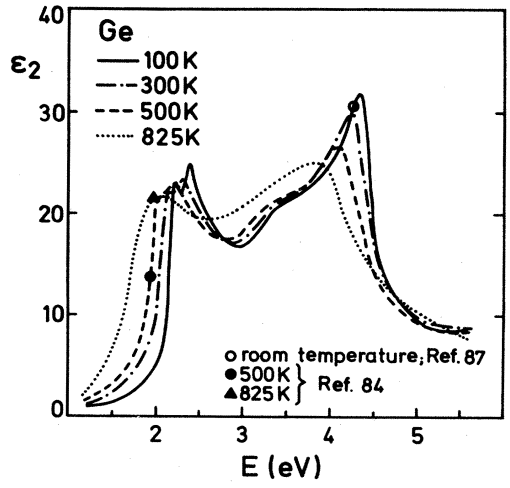

FIG. 2. Imaginary part (ϵ_2) of the pseudodielectric function of Ge. The symbols are the same as in Fig. 1.

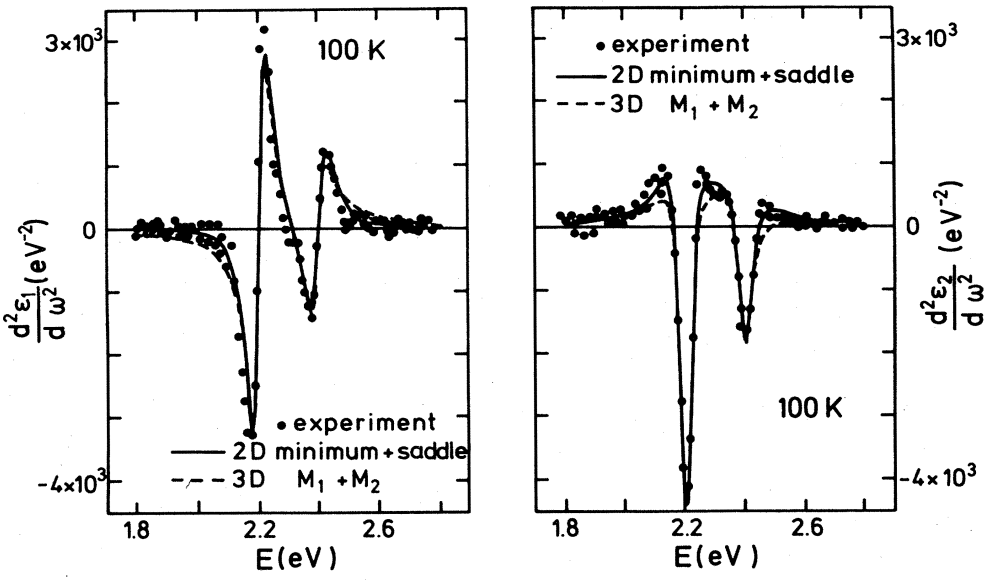

FIG. 3. Second derivatives with respect to the photon energy of the real ($d^2\epsilon_1/d\omega^2$) and imaginary ($d^2\epsilon_2/d\omega^2$) parts of the dielectric constant of Ge at 100 K near the E_1 and $E_1+\Delta_1$ critical points. The points represent experimental data, the solid line represents the best fit with a mixture of a two-dimensional minimum and a saddle point, and the dashed line represents the best fit to a mixture of three-dimensional M_1 and M_2 critical points.

spond to a mixture of a 2D minimum and a saddle point which can be represented by[116,128]

$$\epsilon \sim C - \ln(E-\omega-i\Gamma)e^{i\phi}\,, \tag{1}$$

with the angle ϕ giving the amount of mixture ($0<\phi<\pi/2$). E is the CP energy and Γ the broadening parameter. The dashed lines correspond to a mixture of a 3D M_1 with an M_2 CP, which can be written as[116,128]

$$\epsilon \sim C - (\omega-E+i\Gamma)^{1/2}e^{i\phi}\,, \tag{2}$$

with $0<\phi<\pi/2$. The E_1 and $E_1+\Delta_1$ structures are fitted simultaneously; a fixed SO splitting of 187 meV has been used in the entire range of temperatures and the angle ϕ has been forced to be the same for both transitions.

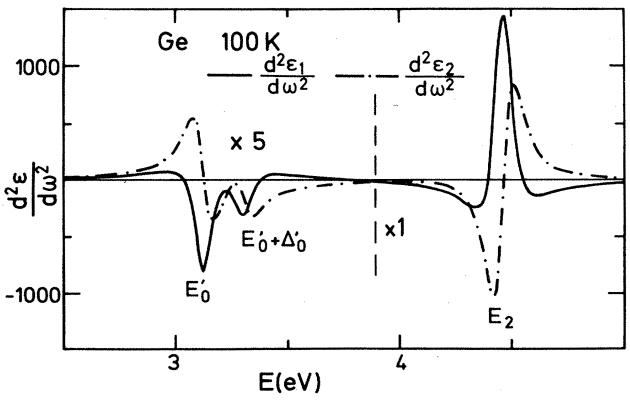

FIG. 4. Fit to the second derivatives with respect to the photon energy of the real and imaginary part of the dielectric function of Ge at 100 K near the E_0', $E_0'+\Delta_0'$, and E_2 critical points. The region corresponding to the E_0' structure is enlarged by a factor of 5. The quality of the fits is comparable to that of Fig. 3.

In Fig. 4 we display the best fit of our data at 100 K to a mixture of a 3D M_0 with a M_1 CP [$-\pi/2<\phi<0$ in Eq. (2)] for the E_0' and $E_0'+\Delta_0'$ structures (these are enlarged by a factor of 5) and a mixture of a 2D saddle point with a maximum for the E_2 CP [$\pi/2<\phi<\pi$ in Eq. (1)]. The solid line corresponds to $d^2\epsilon_1/d\omega^2$ and the dashed one to $d^2\epsilon_2/d\omega^2$. We plot in Fig. 5 the values of $\tan\phi$ for the E_1 transition obtained from our fits versus temperature.

Figure 6 shows the energy position of the E_1, E_2, and E_0' (i.e., the mean value of the E_0' and $E_0'+\Delta_0'$ transitions), as a function of temperature. $E_1+\Delta_1$ runs parallel to E_1, displaced by $\Delta_1=187\pm3$ meV to higher energies, as imposed by the fitting procedure.

The results show a linear dependence of the gaps on temperature at high temperature and a quadratic one at low temperature. The solid lines correspond to the best fit to our data with Varshni's empirical formula:[117]

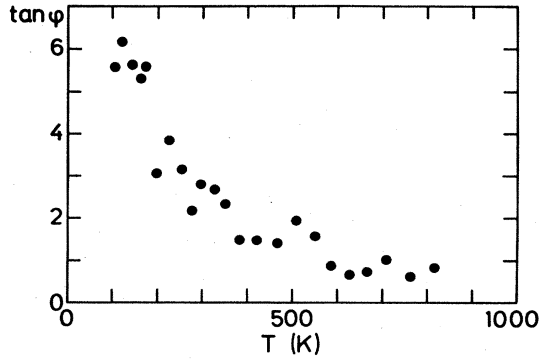

FIG. 5. Dependence on temperature (T) of the excitonic parameter ϕ defined in Eq. (1) for the E_1 critical point of Ge.

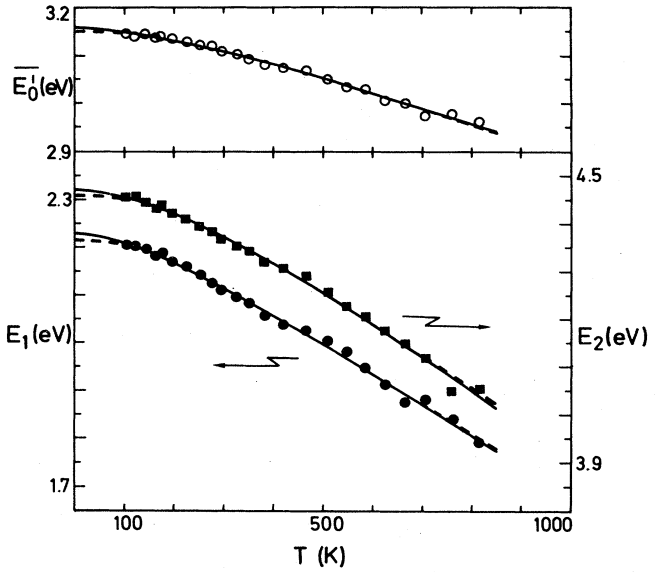

FIG. 6. Dependence on temperature of the critical-point energies of Ge. Solid circles: E_1 critical point (scale on the left). Squares: E_2 critical point (scale on the right). Open circles: $\overline{E_0'}$ defined as average of E_0' and $E_0'+\Delta_0'$ critical points. Solid lines represent the best fits of the data to Eq. (3). Dashed lines correspond to the best fits to Eq. (4).

$$E = a - \frac{\alpha T^2}{\beta + T} . \tag{3}$$

The values of a, α, and β for the E_1, $\overline{E_0'}$, and E_2 critical points obtained from 2D fits together with E_2 obtained from a 1D fit to the second derivatives are listed in Table I with the corresponding uncertainties representing 95% reliability. In this table the values of the parameters for the indirect fundamental gap (E_i) from Refs. 117 and 130 are also presented.

We were also able to fit these data to an expression where the energy thresholds decrease proportional to Bose-Einstein statistical factors for phonon emission plus absorption:

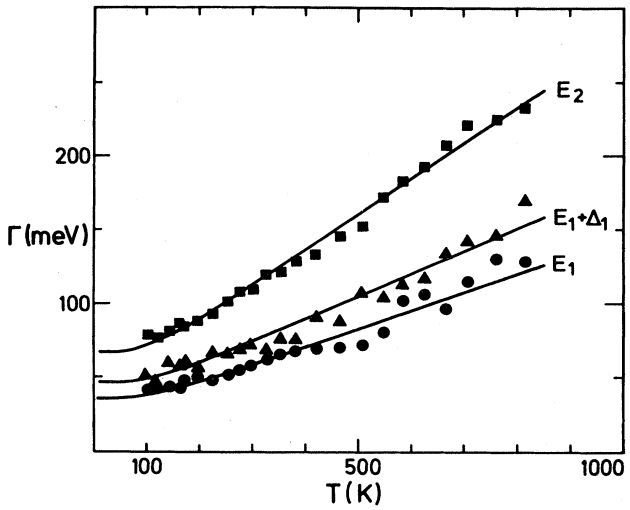

FIG. 7. Dependence of critical-point broadening parameters on temperature. Solid circles: broadening parameter (Γ) for the E_1 transition. Triangles: Γ corresponding to $E_1+\Delta_1$. Squares: Γ for the E_2 singularity. Solid lines represent the best fits of the data to Eq. (5).

$$E = a - b\left[1 + \frac{2}{e^{\Theta/T}-1}\right] . \tag{4}$$

The parameters, again with their corresponding uncertainties, are listed in Table II. The Lorentzian broadening parameter Γ for the E_1 (circles), $E_1+\Delta_1$ (triangles), and E_2 (squares) CP's are displayed in Fig. 7. The solid lines represent our best fit to the data using the formula

$$\Gamma = \Gamma_0\left[1 + \frac{2}{e^{\Theta/T}-1}\right] + \Gamma_1 . \tag{5}$$

Γ_1 represents a fictitious broadening attributable to the approximation used in describing the CP with Eqs. (1) and (2). Due to the uncertainties present in Γ, especially at high temperatures, we have forced Θ to have the same values as those obtained for the corresponding CP ener-

TABLE I. Values of the parameters a, α, and β obtained by fitting the critical-point energy (E) vs temperature (T) to the equation $E = a - \alpha T^2/(T+\beta)$. 2D: two-dimensional critical point. 1D: one-dimensional critical point. $\overline{E_0'}$: average of E_0' and $E_0'+\Delta_0'$ transitions. E_i: indirect gap.

	a (eV)	α (10^{-4} eV K^{-1})	β (K)
E_1(2D)	2.22 ±0.01[a]	6.8±0.8[a]	240±140[a]
$\overline{E_0'}$(2D)	3.159±0.008[a]	3.6±0.7[a]	344±244[a]
E_2(2D)	4.46 ±0.01[a]	8.3±1.0[a]	471±256[a]
E_2(1D)	4.448±0.008[a]	6.8±0.7[a]	319±120[a]
E_i	0.741[b]	4.561[b]	210[b]
		4.7±0.3[c]	235±40[c]

[a]Present work.
[b]Reference 117.
[c]Reference 130.

TABLE II. Values of the parameters a, b, and Θ obtained by fitting the critical-point energy (E) vs temperature (T) to the equation $E=a-b[1+2/(e^{\Theta/T}-1)]$. 2D: two-dimensional. 1D: one-dimensional. $\overline{E_0'}$: average of E_0' and $E_0'+\Delta_0'$ transitions.

	a (eV)	b (eV)	Θ (K)
E_1(2D)	2.33±0.03	0.12±0.04	360±120
$\overline{E_0'}$(2D)	3.23±0.02	0.08±0.03	484±136
E_2(2D)	4.63±0.05	0.17±0.06	499±127
E_2(1D)	4.56±0.03	0.13±0.03	429± 84

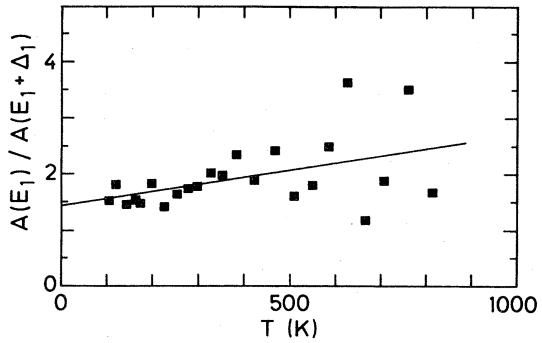

FIG. 8. Dependence on temperature of the ratio of the amplitudes $[A(E_1)/A(E_1+\Delta_1)]$ of the E_1 and $E_1+\Delta_1$ transitions. Solid line represents the best linear fit to the data.

gies. In Table III the parameters Γ_0, Γ_1, and Θ are presented with their uncertainties for the three structures.

Finally in Fig. 8 we show the ratio of the amplitudes of the E_1 and $E_1+\Delta_1$ CP's $[A(E_1)/A(E_1+\Delta_1)]$ versus temperature. A systematic increase of this ratio with T may be inferred from Fig. 8. However, in view of the large scatter of the points at high temperatures, this conclusion should be viewed with caution.

IV. DISCUSSION

In the earlier work of Briggs[73] an increase of n at 1.8 μm with temperature was already indicated. The same result was also found in the single-wavelength ($\lambda=6328$ Å) ellipsometric studies of Refs. 83 and 84 where a monotonic increase of k and an increase of n until $T\sim250$ K followed by a decrease is reported. As can be seen in Fig. 6 of Ref. 85 and in Figs. 1 and 2 of the present work, this fact is due to the shift and broadening of the optical constants directly related to the changes in the band structure with temperature.

In Table IV we list critical-point energies of the main structures present in the optical spectra of Ge above the fundamental gap taken from the literature together with the present data (bottom of the table). The values correspond to room temperature, except those marked with an asterisk, for which temperatures are given in the footnotes. Two authors[23,42] claim to have resolved the M_0 critical points corresponding to the L edge of the BZ with its corresponding SO counterpart; these are the transitions labeled e_1 and $e_1+\Delta_1$. They have not been identified here nor in many other references. Slightly different temperature coefficients for the e_1 and E_1 transitions are reported in Ref. 42, which should help to separate them in our temperature-dependent measurement.

TABLE III. Values of the parameters Γ_0, Γ_1, and Θ obtained by fitting the Lorentzian broadening parameter (Γ) vs temperature (T) to the equation $\Gamma=\Gamma_0[1+2/(e^{\Theta/T}-1)]+\Gamma_1$. 2D: two-dimensional CP. 1D: one-dimensional CP. Θ has been forced to have the same values as in Table II.

	Γ_0 (meV)	Γ_1 (meV)	Θ (K)
E_1(2D)	25±3	12±9	376
$E_1+\Delta_1$(2D)	43±5	9±8	484
E_2(2D)	69±3	8±5	499
E_2(1D)	72±3	31±6	429

A. E_1 and $E_1+\Delta_1$ transitions

As can be seen in Table IV, the CP energy of the E_1 transition found at room temperature in the present work compares well with electroreflectance data (Refs. 37, 39, 42, 56, and 131, the last with a 2D fit to the critical point). In the case of the $E_1+\Delta_1$ transition our energy again compares well with that of Refs. 56 and 131. Larger discrepancies appear in the other cases presumably because the $E_1+\Delta_1$ peak, weaker than E_1, cannot be accurately determined at RT unless a detailed line-shape fit is made.

The two- or three-dimensional character of the E_1 transitions has been profusely discussed in the literature.[53,56,62,116,131] Spectroscopic ellipsometry yields directly the dielectric function, and hence it should be the most appropriate technique to analyse the nature of these critical points. We have carefully investigated the derivative spectra from 2.0 to 2.5 eV. The E_1 and $E_1+\Delta_1$ structures were fitted simultaneously using a mixture of M_1 and M_2 3D CP's [see Eq. (2)] or a mixture of a 2D minimum and a saddle point [see Eq. (1)]. At all temperatures we found a slightly better fit (10%) using line shapes corresponding to 2D CP's. In Fig. 3 the experimental data at 100 K are shown together with both fits, the main differences appearing in the wings of the structures. The weak structure seen at 2.3 eV, also present in electroreflectance,[131] could not be fitted in any case. The presence of an M_0 CP at the edge of the BZ together with an M_1 in the [111] direction has also been proposed (see, e.g., Ref. 39) to explain the line shape of these structures. This would give a line shape similar to that of a two-dimensional minimum. The E_1 and $E_1+\Delta_1$ critical points are *strictly speaking* three dimensional. They correspond to transitions between the Λ_6 and the Λ_{4-5} valence bands to the Λ_1 conduction band.[111] Two possible structures for the corresponding 3D gaps are suggested in the literature. In Ref. 93 a 3D minimum (M_0) at the L point followed by a 3D saddle point along Λ, close to Γ, are

TABLE IV. Critical-point energies of interband transitions in Ge. Values correspond to room temperature, except those marked with *, whose temperature is given in the footnotes.

e_1 (eV)	$e_1+\Delta_1$ (eV)	E_1 (eV)	$E_1+\Delta_1$ (eV)	Δ_1 (meV)	E_0' (eV)	$E_0'+\Delta_0'$ (eV)	E_2 (eV)
2.107[a]	2.294[a]	2.134[a]	2.314[a]	180[a]			
2.05[b]	2.24[b]	2.12[b]	2.32[b]	200[b]	2.80[b]	2.93[b]	
		2.15[c]	2.35[c]	200[c]			
		2.09[d,e]	2.26[d,e]	170[d,e]			
		2.115[f]	2.325[f]	210[f]			
		2.12[g]	2.34[g]	220[g]	3.14[g]	3.33[g]	4.42[g]
		2.087[h]	2.291[h]	204[h]			
		2.065[i]	2.266[i]	201[i]			
		2.09[j]	2.29[j]	200[j]			4.35[j]
					3.10[k]		
					2.92[l]		
					2.983[m]	3.169[m]	
		2.105[n]	2.303[n]	198[n]			
		2.126[o]	2.332[o]	206[o]			
		2.107[p]	2.303[p]	196[p]			
				213[q]			
				175[r]			
				180[s]			
		*2.250[t]	*2.434[t]	*184[t]	*3.006[t]	*3.206[t]	*4.501[t]
		*2.222[u]	*2.420[u]	*198[u]			*4.49[u]
					*3.20[v]		
					*3.0[w]	*3.191[w]	
					*3.015[x]	*3.201[x]	
					*3.123±0.19[y]	*3.309±0.19[y]	
		2.111±0.003[z]	2.298±0.003[z]	187±3[z]			4.368±0.004[z]
							4.346±0.003[α]
					3.110[β]		

[a]Reference 23, extrapolated to 295 K.
[b]Reference 42.
[c]Reference 3.
[d]Reference 44.
[e]Reference 47.
[f]Reference 37.
[g]Reference 39.
[h]Reference 53 with 2D CP.
[i]Reference 53 with 3D CP.
[j]Reference 59.
[k]Reference 59, mean value of E_0' and $E_0'+\Delta_0'$.
[l]Reference 52.
[m]Reference 49.
[n]Reference 131 with 2D CP.
[o]Reference 131 with 3D CP.
[p]Reference 56.
[q]Reference 36.
[r]Reference 26.
[s]Reference 9.
[t]Reference 50 at 10 K.
[u]Reference 71 at 5 K.
[v]Reference 71 at 5 K, mean value of E_0' and $E_0'+\Delta_0'$.
[w]Reference 46 at 83 K.
[x]Reference 49 at 78 K.
[y]Present work at 100 K with 3D CP.
[z]Present work with 2D CP.
[α]Present work with 1D CP.
[β]Present work, mean value of E_0' and $E_0'+\Delta_0'$ with 2D CP.

suggested. These two critical points are nearly degenerate in energy (closer actually than the Γ's found from our fits). Hence, as shown in Fig. 9, their conjunction is difficult to distinguish from a 2D critical point. Reliable recent calculations[115] suggest that the M_0 critical point may not exist at all: Only an M_1 critical point exists at L while the band separation decreases monotonically from L to Γ without reaching a maximum. However, for most of the stretch from L to Γ the bands are nearly parallel and an approximate 2D critical point is also obtained. In view of this we believe the 2D critical point provides at present the most reasonable and internally consistent representation of the E_1 and $E_1+\Delta_1$ transitions.

In order to reduce the number of parameters of the fits, and also to be able to fit together the E_1 and $E_1+\Delta_1$ CP's at elevated temperatures where they have become shoulders (see Fig. 2), we have assumed an SO splitting Δ_1 independent of T. This fact is supported by earlier measurements[25,34,44,69] and by the intraatomic nature of the SO splitting. The value used, $\Delta_1=187$ meV, was found at 100 K.

In Table V the Lorentzian broadening parameters Γ obtained from this work are listed together with values found in the literature, again at room temperature unless marked with an asterisk. The broadenings depend on the type of CP assumed. The Γ's of the E_1, $E_1+\Delta_1$ transitions are a factor ~ 1.5 smaller for a fit with a 3D than with a 2D critical point. Our values at RT obtained with a fit to a 2D CP agree with those of Refs. 53 and 131.

Excitonic effects in the vicinity of the E_1 and $E_1+\Delta_1$

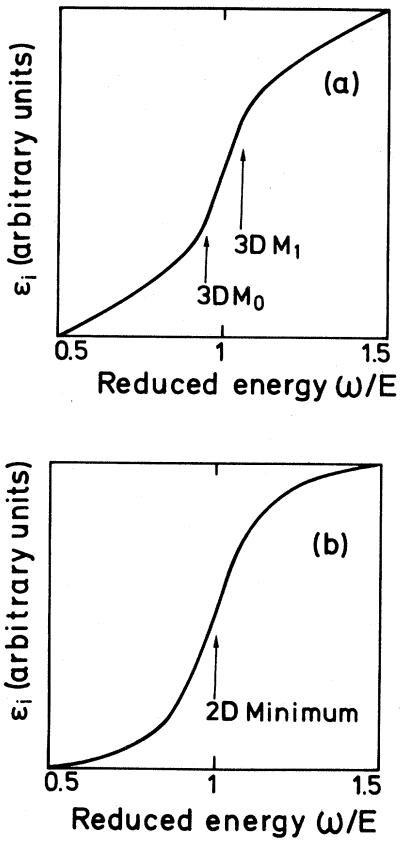

FIG. 9. (a) Calculated density of states corresponding to a conjunction of M_0 and M_1 3D critical points. (b) Density of states corresponding to a broadened 2D minimum critical point. A reduced broadening parameter $\Gamma/E=0.11$ is used for the 2D CP's and $\Gamma/E=0.025$ for each 3D CP's.

transitions in Ge have been reported in the literature.[55,56,61,69,79,128] A sharp dropoff of $\epsilon_2(\omega)$ above E_1 and also above $E_1+\Delta_1$ is the most characteristic of these effects which can be described as the interference of a discrete two-dimensional exciton with a quasicontinuous background.[132,133] A simple qualitative description of these effects can be made by multiplying the one-electron dielectric constant by a phase factor $e^{i\phi}$.[128] We have used this procedure with ϕ as an adjustable parameter in our fit. The phase angle ϕ plotted in Fig. 5 decreases rapidly with increasing temperature, an empirical fact which suggests a decrease in excitonic effects as the temperature is raised. The angles, as chosen by us, represent the amount of 2D saddle point added to a minimum for the fit of the measured line shape. The value of $\phi=65°$ at room temperature agrees well with the electroreflectance value $\phi=60°$.[82] The reduction of exciton interaction of about a factor of 3 between 100 and 300 K agrees also with the reduction found in thermoreflectance.[69]

The 2D fits of Fig. 3 were performed with the functions

$$\left[\frac{d^2\epsilon}{d\omega^2}\right]_{E_1}=-\frac{A_{E_1}e^{i\phi}}{(E_1-\hbar\omega-i\Gamma)^2}\,,$$
$$\left[\frac{d^2\epsilon}{d\omega^2}\right]_{E_1+\Delta_1}=-\frac{A_{E_1+\Delta_1}e^{i\phi}}{(E_1+\Delta_1-\hbar\omega-i\Gamma)^2}\,. \tag{6}$$

Within the microscopic uncorrelated electrons model of Ref. 134 the prefactors A_{E_1} and $A_{E_1+\Delta_1}$ are given by

$$A_{E_1}\simeq 44\frac{E_1+\Delta_1/3}{a_0E_1^2}\,,$$
$$A_{E_1+\Delta_1}\simeq 44\frac{E_1+2\Delta_1/3}{a_0(E_1+\Delta_1)^2}\,, \tag{7}$$

where a_0 is the lattice constant in Å and the energies are in eV. For the 2D fit of Fig. 3 at 100 K we find $A_{E_1}=8.1$ and $A_{E_1+\Delta_1}=5.2$ while Eq. (6) predicts $A_{E_1}=3.6$ and $A_{E_1+\Delta_1}=3.2$. The agreement between the calculated and the experimental values is reasonable in view of the crude-

TABLE V. Lorentzian broadening parameters of interband transitions in Ge. Values correspond to room temperature, except those marked with * whose temperatures are given in the footnotes.

$\Gamma(E_1)$ (meV)	$\Gamma(E_1+\Delta_1)$ (meV)	$\Gamma(E_0')$ (meV)	$\Gamma(E_0'+\Delta_0')$ (meV)	$\Gamma(E_2)$ (meV)
*27[a]	*44[a]	*33[a]	*33[a]	*66[a]
79[b]	95[b]			
59[c]	74[c]			
44[d]	62[d]			
53[e]	69[e]			
38[f]	52[f]			
*41± 3[g]	*55± 7[g]			*78± 2[g]
*28± 2[h]	*38± 3[h]	*60±25[h]	*65±30[h]	
				*108± 5[i]
58± 5[j]	73±10[j]			109± 4[j]
				148± 6[k]

[a]Reference 51 at 10 K with 2D CP.
[b]Reference 56.
[c]Reference 131 with 2D CP.
[d]Reference 131 with 3D CP.
[e]Reference 53 with 2D CP.
[f]Reference 53 with 3D CP.
[g]Present work at 100 K with 2D CP.
[h]Present work at 100 K with 3D CP.
[i]Present work at 100 K with 1D CP.
[j]Present work with 2D CP.
[k]Present work with 1D CP.

ness of the theory used. Some improvement of this theoretical estimate is possible by including the "linear terms in $k_\perp$" ($\perp$ means perpendicular to $\{111\}$) discussed in Ref. 135. These terms, which are linear in $k_\perp$ only in the absence of spin-orbit interaction, increase the transverse mass for the E_1 gap and decrease that for the $E_1+\Delta_1$ gap according to Eq. (4) of Ref. 135. For an average matrix element $|\Pi|=0.1$ bohr^{-1}, which we have calculated for Ge following the method of Ref. 135, we find $A_{E_1}=4.1$, $A_{E_1+\Delta_1}=2.5$. The calculated ratio of these A's is 1.64 which compares well with the experimental one of 1.55 at 100 K (Fig. 8). The difference between measured and calculated A's can be attributed to excitonic interaction.[136]

The solid line in Fig. 8 gives the least-squares fit to the experimental points:

$$\frac{A_{E_1}}{A_{E_1+\Delta_1}}=1.75+(1.3\pm0.5)\times10^{-3}T\ . \tag{8}$$

In view of the large error in the temperature coefficient of Eq. (8), and the large scatter of the experimental points in Fig. 8, it is difficult to attribute a physical significance to Eq. (8). In any case we have not found a physical mechanism which would explain an increase in $A_{E_1}/A_{E_1+\Delta_1}$.

The solid lines plotted in Fig. 6 correspond to the best fit to Eq. (3).[117] The only basis for this expression is the fact that the energy gap is quadratic in T at low temperatures and linear at high temperatures. The parameters of the fit are listed in Table I. β should be an estimate of the Debye temperature which in Ge has a value of 374 K (at RT). We also found that an equally good fit can be obtained with an expression proportional to the sum of the statistical factors for phonon absorption and emission [Eq. (4)], an expression which is more palatable from the theoretical view point. A similar expression has already been employed to analyze the temperature dependence of the fundamental gap in diamond, silicon, and germanium.[137] The values of the fit parameters for 95% reliability are shown in Table II. The parameter Θ represents the mean temperature of the phonons taking part in the scattering process. The large value of Θ indicates that acoustic phonons tend to contribute less than the optic ones at high temperatures, a fact which is also borne out by calculations for the fundamental gap.[111] In Table VI we present the linear temperature coefficients of the different gaps found in the literature together with results from a linear fit to our data between 100 and 300 K. We have made two fits, one taking as the critical point the peaks in the reflectivity obtained from our ϵ data and the other with the critical-point energies from our line-shape analysis. For the E_1 transition both fits agree within the error bars and also agree with the other values in the literature. The broadening parameters shown in Fig. 7 were fitted with Eq. (5). The fit parameters are listed in Table III. The mean temperature Θ of the phonons taking part in the scattering process was forced to have the same value as obtained for the fit to the CP energies. A more accurate determination of the broadening parameters which would allow us to distinguish between Debye-Waller and "self-energy" terms in its temperature dependence would be desirable. The Debye-Waller term does not contribute to the imaginary part of the changes in the energy bands, the self-energy term is the only one responsible for the increase in the broadening parameter. Hence different phonons may have a different weight in the contribution to the imaginary part than to the real part of the temperature effects. Using the fact that the temperature dependence of the upper valence-band states are nearly the same for all $\vec{k}$ (Ref. 60) and also that the temperature coefficients of the different gaps are rather similar (see Table VI), we have made a crude estimate of the mean temperature of the phonons contributing to the broadening in the high-T limit using the data from Figs. 2 and 3 of Ref. 111, which, however, apply, strictly speaking, only to E_0. Calculations for other gaps are not yet available. Figures 2 and 3 of Ref. 111 indicate that the conduction-band broadening is much smaller than the valence-band counterpart. We thus neglect the former. The average phonon frequency appropriate to the high-temperature limit is obtained by averaging ω^{-2} with the weighting function $\omega g^2F(\omega)$, where $g^2F(\omega)$ is the self-energy part of the spectral function (Fig. 2 of Ref. 111). Following this procedure we obtain an average phonon frequency of 260 K, somewhat smaller than those used for our fits. We obtain from our measurements a linear coefficient of $\Gamma(E_1)$ between 100 and 300 K of $(8\pm2)\times10^{-5}$ eV/K, somewhat larger than the value $(4\pm1)\times10^{-5}$ eV/K from Ref. 69. We note that the values of $\Gamma_1\simeq10$ meV (Table III) impose an upper limit to the possible separation of M_0 and M_1 critical points which may contribute to the E_1 transition.

B. E_0' transitions

At low temperatures we are able to resolve the E_0' and $E_0'+\Delta_0'$ CP's. The $E_0'+\Delta_0'+\Delta_0$ critical point was too weak to be observed.[42,50] Our CP parameters at 100 K for the energy and broadening (found with a mixture of M_0 and M_1 3D CP's) are somewhat larger than those in Refs. 42 and 50 but agree with them within experimental error. To obtain the temperature dependence of these gaps we have fitted both of them together using a single two-dimensional CP. The energy of $\overline{E_0'}$ (average of E_0' and $E_0'+\Delta_0'$) are plotted at the top of Fig. 6 versus temperature. The coefficient of the fits to Eqs. (3) (shown as the solid line in Fig. 6) and (4) can be seen in Tables I and II, respectively. The values of β and Θ are within the margins of error in the same range as those of E_1. However, the linear coefficient corresponding to high temperatures is smaller. With a linear fit to the data we found a temperature coefficient of -1.8×10^{-4} eV/K. We have calculated the contribution of thermal expansion to the temperature coefficient of this gap and found it to be negligible. If we assume that the temperature dependence of the Γ_{15} state in Ge is the same as in silicon, the E_0' gap in Ge should have a theoretical linear temperature coefficient (from 100 to 600 K) of -2.2×10^{-4} eV/K (see Fig. 6 in Ref. 111) in good agreement with our experiments. We do not present values for the Γ of the E_0' as a function of temperature since those found from the fit are strongly affected by the proximity of $E_0'+\Delta_0'$.

TABLE VI. Linear temperature coefficients of intraband transitions in Ge. All values in 10^{-4} eV/K.

$-dE_0/dT$	$-de_1/dT$	$-dE_1/dT$	$-d(E_1+\Delta_1)/dT$	$-dE_0'/dT$	$-dE_2/dT$
4.5[a]		4.2[d]			1.8±0.5[d,f]
3.7[b]		4.2 ±0.4[e,f,g]	4.2±0.4[e]		2.4±0.4[g]
4±0.2[c]		3.9[h]			1.2[h]
		4.15±0.2[i]			
		4.4 ±0.3[j]			
		4.1 ±0.2[k,l]	4.3±0.2[k]		3.9±0.9[l]
		3.89±0.02[m]			
		4.3[n]	4.5[n]		
		3.9±0.3[o]	4.5±0.2[o]		
		5.2[p]	5.5[p,q]		2.9±0.3[o]
		4.8[q]			
	5.47±0.02[r]	3.89±0.02[r]		1.4[s]	
		4.5 ±0.3[t]			2.9±0.3[t]
		4.8 ±0.2[u]		1.8[u]±0.1	
					4.6±0.2[u]
Theory		3.7[l]			2.85[l]
					3.3[v]
				2.2[w]	

[a]See. F. S. Goucher and H. B. Briggs, in J. Bardeen and W. Schockley, Phys. Rev. **80**, 72 (1950).
[b]Reference 36.
[c]Reference 60.
[d]Reference 25.
[e]M. Cardona, J. Appl. Phys. **32**, 2151 (1961).
[f]M. Cardona and D. L. Greenaway, Phys. Rev. **125**, 1291 (1962).
[g]Reference 71.
[h]Reference 27.
[i]Reference 3.
[j]Reference 9.
[k]Reference 69.
[l]Reference 60.
[m]Reference 23.
[n]Reference 34.
[o]Reference 62.
[p]Reference 44.
[q]Reference 47.
[r]Reference 23.
[s]Reference 49.
[t]Present work from 100 to 300 K obtained from peak in reflectivity.
[u]Present work from 100 to 300 K obtained from fit of $d^2\epsilon/d\omega^2$ to 2D CP.
[v]Reference 106 calculated for the Penn gap.
[w]Reference 111.

C. E_2 transition

The nature of the E_2 transition is more complicated since it does not correspond to a single, well-defined critical point. This structure has been attributed to transitions at X and along the Σ direction,[93] to an extended region in the BZ where transitions in the Σ direction and along the $L-U$ line are important,[96] and to a small region centered at $(2\pi/a)(0.77, 0.29, 0.16)$.[99] However, more recently,[115] and also in Ref. 97, it is felt to originate from a region in the Γ-X-U-L plane near $(2\pi/a)(\frac{3}{4}, \frac{1}{4}, \frac{1}{4})$. This structure could be reasonably fitted at room temperature, using either a 1D maximum, as was done for Si,[138] or a 3D M_2 CP. However, we found that at low temperatures a better fit is achieved with a mixture of a 2D saddle point and a 2D maximum. This fact has also been found in low-temperature measurements for α-Sn.[139] The phase angle shows also a decrease with increasing temperature. Because of the complicated character of this transition we cannot conclude whether this effect is excitonic or it is simply due to different temperature shifts of the electron states contributing to the transition. The CP energies and broadening parameters of this transition are shown in Figs. 6 and 7 (squares) versus temperature. The solid lines correspond to the best fits to Eq. (3) (energy shifts) and Eq. (5) (broadenings); the coefficients of the fits are shown in Tables I, II, and III. We found the same energy-shift coefficients, within error, as for the E_1 transition. However, we found that the effect of temperature on broadening in the case of E_2 is larger than for the E_1 and $E_1+\Delta_1$ CP's. We want to point out that this effect depends on the dimensionality of the CP chosen for the fit. The best representation of this structure over the entire temperature range seems to be obtained with a two-dimensional CP.

In Table VI we list the linear coefficients of this transition obtained in the (100—300)-K range. A value of $-(2.9\pm0.3)\times10^{-4}$ eV/K is obtained for the peak in the reflectivity (calculated from our ϵ values). (This peak is commonly but erroneously used in the literature as characteristic of the CP position.) This temperature coefficient is in good agreement with the values in the litera-

ture. However, a much larger coefficient $-(4.6\pm0.2)\times10^{-4}$ eV/K is obtained from our complete line-shape analysis. The discrepancy is due to the fact that shifts and broadenings appear mixed in the temperature coefficient of the reflectivity peak. The practice of associating CP energies with peaks in ϵ_2, reflection, or modulation spectra without a line-shape analysis can lead to substantial errors and should be avoided.

V. CONCLUSIONS

We have measured the effect of temperature on the optical critical points of germanium. Accurate dielectric function data are presented in the temperature range of 100 to 850 K. The critical-point energies and Lorentzian broadening parameters of the E_1, $E_1+\Delta_1$, E_0', and E_2 structures have been obtained by analysis of the numerically calculated second-derivative spectra of the original data. A large decrease of excitonic effects at the E_1 and $E_1+\Delta_1$ gaps was found with increasing temperature. To our knowledge, this is the first systematic investigation of the effect of temperature on the dielectric function of a semiconductor, in particular, on the broadening of the optical structures. Line shapes corresponding to two-dimensional critical points are found to be the best representation of the E_1 and $E_1+\Delta_1$ transitions.

ACKNOWLEDGMENTS

We would like to thank E. Schönherr for the crystal growth, H. Höchst and W. Neu for help with the construction of the cryostat, G. Kisela for sample preparation, and H. Bleder and H. Birkner for help with the construction of the ellipsometer. We would also thank H. Hirt, M. Siemers, and P. Wurster for expert technical help.

*On leave from Aristotle University of Thessaloniki, First Laboratory of Physics, Thessaloniki, Greece.

[1]W. H. Brattain and H. B. Briggs, Phys. Rev. **75**, 1705 (1949).

[2]O. P. Rustgi, J. S. Nodvik, and G. L. Weissler, Phys. Rev. **122**, 1131 (1961).

[3]M. Cardona and G. Harbeke, J. Appl. Phys. **34**, 813 (1963).

[4]M. Cardona, W. Gudat, B. Sonntag, and P. Y. Yu, in *Proceedings of the 10th International Conference on the Physics of Semiconductors,* edited by S. P. Keller, J. C. Hensel, and F. Stern (United States Atomic Energy Commission, Cambridge, Mass., 1970), p. 209.

[5]M. Becker and H. Y. Fan, Phys. Rev. **76**, 1531 (1949).

[6]W. Paul and D. M. Warschauer, J. Phys. Chem. Solids **5**, 89 (1958); W. Paul, *ibid.* **8**, 196 (1959).

[7]M. Cardona, W. Paul, and H. Brooks, J. Phys. Chem. Solids **8**, 204 (1959).

[8]M. Cardona and W. Paul, J. Phys. Chem. Solids **17**, 138 (1960).

[9]G. Harbeke, Z. Naturforsch. Teil A **19**, 548 (1964).

[10]G. G. MacFarlane and V. Roberts, Phys. Rev. **97**, 1714 (1955); G. G. MacFarlane, T. P. McLean, J. E. Quarrington, and V. Roberts, *ibid.* **108**, 1377 (1957); J. Phys. Chem. Solids **8**, 388 (1959).

[11]W. C. Dash and R. Newmann, Phys. Rev. **99**, 1151 (1955).

[12]R. Braunstein, A. R. Moore, and F. Herman, Phys. Rev. **109**, 695 (1958).

[13]M. V. Hobden, J. Phys. Chem. Solids **23**, 821 (1962).

[14]R. A. Smith, S. Zwerdling, S. N. Dermatis, and J. P. Theriault, in *Proceedings of the 9th International Conference on the Physics of Semiconductors, Moscow, 1968* (Publishing House of the Academy of Sciences of the USSR, Leningrad, 1968), p. 149.

[15]G. Chiarotti, G. Del Signore, and S. Nannarone, Phys. Rev. Lett. **21**, 1170 (1968); G. Chiarotti, S. Nannarone, R. Pastore, and P. Chiaradia, Phys. Rev. B **4**, 3398 (1971).

[16]S. Zwerdling and B. Lax, Phys. Rev. **106**, 51 (1957); S. Zwerdling, B. Lax, and L. M. Roth, *ibid.* **108**, 1402 (1957); S. Zwerdling, L. M. Roth, and B. Lax, *ibid.* **109**, 2207 (1958).

[17]D. F. Edwards, V. J. Lazazzera, and C. W. Peters, in *Proceedings of the International Conference on the Physics of Semiconductors, Prague, 1960* (Publishing House of the Czechoslovak Academy of Sciences, Prague, 1961), p. 335.

[18]B. P. Zakharchenya, R. P. Seysyan, and A. V. Varfolomeev, in *Proceedings of the 9th International Conference on the Physics of Semiconductors, Moscow, 1968,* Ref. 14, p. 269.

[19]A. Frova and P. Handler, Phys. Rev. **137**, A1857 (1965); A. Frova, P. Handler, F. A. Germano, and D. E. Aspnes, *ibid.* **145**, 575 (1966).

[20]Y. Hamakawa, F. A. Germano, and P. Handler, J. Phys. Soc. Jpn. Suppl. **121**, 111 (1966); Y. Hamakawa, F. A. Germano, and P. Handler, Phys. Rev. **167**, 703 (1968).

[21]Q. H.-T. Vrehen, Phys. Rev. **145**, 675 (1966).

[22]E. Adler and E. Erlbach, Phys. Rev. Lett. **16**, 87 (1966).

[23]F. R. Kessler and K. Dettmer, Phys. Status Solidi B **51**, 79 (1972).

[24]J. Tauc and E. Antončik, Phys. Rev. Lett. **5**, 253 (1960); J. Tauc and A. Abrahám, J. Phys. Chem. Solids **20**, 190 (1961); J. Tauc and A. Abrahám, in *Proceedings of the International Conference on the Physics of Semiconductors, Prague, 1960* (Publishing House of the Czechoslovak Academy of Sciences, Prague, 1961), p. 375.

[25]M. Cardona and H. S. Sommer, Jr., Phys. Rev. **122**, 1382 (1961).

[26]T. M. Donovan, E. J. Ashley, and H. E. Bennett, J. Opt. Soc. Am. **53**, 1403 (1963).

[27]A. Abrahám, J. Tauc, and B. Velický, Phys. Status Solidi **3**, 767 (1963).

[28]L. Pajasová, Solid State Commun. **4**, 619 (1966).

[29]L. Marton and J. Toots, Phys. Rev. **160**, 602 (1967).

[30]R. Zallen and W. Paul, Phys. Rev. **155**, 703 (1967).

[31]D. D. Sell and E. O. Kane, Phys. Rev. B **5**, 417 (1972).

[32]H. R. Philipp and E. A. Taft, Phys. Rev. **113**, 1002 (1959); H. R. Philipp and H. Ehrenreich, *ibid.* **129**, 1550 (1963).

[33]T. Sasaki, J. Phys. Soc. Jpn. **18**, 701 (1963).

[34]E. Schmidt, Phys. Status Solidi **27**, 57 (1968).

[35]B. O. Seraphin, in *Proceedings of the 7th International Conference on the Physics of Semiconductors, Paris, 1964,* edited by M. Hulin (Dunod, Paris, 1964), p. 165; B. O. Seraphin and R. B. Hess; Phys. Rev. Lett. **14**, 138 (1965).

[36]B. O. Seraphin, R. B. Hess, and N. Bottka, J. Appl. Phys. **36**, 2242 (1965).
[37]K. L. Shaklee, F. H. Pollak, and M. Cardona, Phys. Rev. Lett. **15**, 883 (1965).
[38]M. Cardona, F. H. Pollak, and K. L. Shaklee, J. Phys. Soc. Jpn. Suppl. **21**, 89 (1966); M. Cardona, K. L. Shaklee, and F. H. Pollak, Phys. Lett. **23**, 37 (1966).
[39]M. Cardona, K. L. Shaklee, and F. H. Pollak, Phys. Rev. **154**, 696 (1967).
[40]B. Batz, Solid State Commun. **4**, 241 (1966).
[41]A. K. Gosh, Solid State Commun. **4**, 565 (1966).
[42]A. K. Gosh, Phys. Rev. **165**, 888 (1968).
[43]Y. Hamakawa, P. Handler, and F. A. Germano, Phys. Rev. **167**, 709 (1968).
[44]Y. Hamakawa, T. Nishino, and J. Yamaguchi, in *Proceedings of the 9th International Conference on the Physics of Semiconductors, Moscow, 1968,* Ref. 14, p. 384.
[45]J. E. Fischer, D. S. Kyser, and N. Bottka, Solid State Commun. **7**, 1821 (1969).
[46]J. E. Fischer, in *Proceedings of the 10th International Conference on the Physics of Semiconductors,* edited by S. P. Keller, and J. C. Hensel, and F. Stern (United States Atomic Energy Commission, Cambridge, Mass., 1970), p. 427.
[47]T. Nishino and Y. Hamakawa, J. Phys. Soc. Jpn. **26**, 403 (1969).
[48]D. E. Aspnes and A. Frova, Phys. Rev. B **2**, 1037 (1970); D. E. Aspnes and J. E. Rowe, in *Proceedings of the 10th International Conference on the Physics of Semiconductors,* edited by S. P. Keller, J. C. Hensel, and F. Stern (United States Atomic Energy Commission, Cambridge, Mass., 1970), p. 422; D. E. Aspnes, Surf. Sci. **37**, 418 (1973).
[49]D. E. Aspnes, Phys. Rev. Lett. **28**, 913 (1972).
[50]D. E. Aspnes, Phys. Rev. Lett. **31**, 230 (1973).
[51]D. E. Aspnes, Phys. Rev. B **12**, 2297 (1975).
[52]T. M. Donovan, J. E. Fischer, J. Matsuzaki, and W. E. Spicer, Phys. Rev. B **3**, 4292 (1971).
[53]S. Koeppen, P. Handler, and S. Jasperson, Phys. Rev. Lett. **27**, 265 (1971).
[54]C. Alibert, in *Proceedings of the Autumn School on Modulation Spectroscopy,* edited by R. Enderlein (Zentralinstitut für Elektronenphysik der Akademie der Wissenschaften der DDR, Berlin, 1977), p. 248.
[55]M. Chandrasekhar and F. H. Pollak, Phys. Rev. B **15**, 2127 (1977).
[56]J. Humlíček, Phys. Status Solidi B **86**, 303 (1978).
[57]W. E. Engeler, H. Fritzsche, M. Garfinkel, and J. J. Tiemann, Phys. Rev. Lett. **14**, 1069 (1965).
[58]U. Gerhardt, Phys. Rev. Lett. **15**, 401 (1965); U. Gerhardt, Phys. Status Solidi **11**, 801 (1965).
[59]J. Takizawa, H. Fukutani, and G. Kuwabara, J. Phys. Soc. Jpn. **35**, 543 (1973).
[60]D. Auvergne, J. Camassel, H. Mathieu, and M. Cardona, Phys. Rev. B **9**, 5168 (1974).
[61]M. Chandrapal and F. H. Pollak, Solid State Commun. **18**, 1263 (1976).
[62]J. Musilová, Phys. Status Solidi B **101**, 85 (1980).
[63]W. E. Engeler, H. Garfinkel, and J. J. Tiemann, Phys. Rev. Lett. **16**, 239 (1966); W. E. Engeler, M. Garfinkel, and J. J. Tiemann, Phys. Rev. **155**, 693 (1967).
[64]F. H. Pollak and M. Cardona, Phys. Rev. **172**, 816 (1968).
[65]S. H. Groves, C. R. Pidgeon, and J. Feinleib, Phys. Rev. Lett. **17**, 643 (1966).
[66]R. Ranvaud, C. Alibert, A. M. Joullie, and M. Cardona, in *Proceedings of the 12th International Conference on the Physics of Semiconductors, Stuttgart, 1974,* edited by M. H. Pilkuhn (Teubner, Stuttgart, 1974), p. 536; C. Alibert, A. M. Joullie, E. Monteil, A. Joullie, and R. Ranvaud, in *Proceedings of the 13th International Conference on the Physics of Semiconductors, Rome, 1976,* edited by F. G. Fumi (North-Holland, Amsterdam, 1976), p. 1039.
[67]R. L. Aggarwal, L. Rubin, and B. Lax, Phys. Rev. Lett. **17**, 8 (1966).
[68]J. G. Mavroides, M. S. Dresselhaus, R. L. Aggarval, and G. F. Dresselhaus, J. Phys. Soc. Jpn. Suppl. **21**, 184 (1966).
[69]E. Schmidt, Phys. Status Solidi B **45**, K39 (1971).
[70]I. Balslev, Phys. Rev. **143**, 636 (1966).
[71]R. R. L. Zucca and Y. R. Shen, Phys. Rev. B **1**, 2668 (1970).
[72]R. Braunstein and M. Welkowsky, in *Proceedings of the 10th International Conference on the Physics of Semiconductors,* edited by S. P. Keller, J. C. Hensel, and F. Stern (United States Atomic Energy Commission, Cambridge, Mass., 1970), p. 439.
[73]H. B. Briggs, Phys. Rev. **77**, 287 (1949).
[74]C. D. Salzberg and J. L. Villa, J. Opt. Soc. Am **47**, 244 (1957).
[75]F. Lukeš and E. Schmidt, in *Proceedings of the International Conference on the Physics of Semiconductors, Prague, 1960* (Publishing House of the Czechoslovak Academy of Sciences, Prague, 1961), p. 371.
[76]R. F. Potter, J. Phys. Soc. Jpn. Suppl. **21**, 107 (1966); R. F. Potter, Phys. Rev. **150**, 562 (1966).
[77]E. Schmidt, Appl. Opt. **8**, 1905 (1969).
[78]R. J. Archer, Phys. Rev. **110**, 354 (1958).
[79]D. T. F. Marple and H. Ehrenreich, Phys. Rev. Lett. **8**, 87 (1962).
[80]F. Meyer, E. E. de Kluizenaar, and G. A. Bootsma, Surf. Sci. **27**, 88 (1971).
[81]G. Jungk, Phys. Status Solidi B **44**, 239 (1971); **67**, 85 (1975); in *Proceedings of the Autumn School on Modern Spectroscopy,* Ref. 54, p. 176.
[82]D. E. Aspnes, Phys. Rev. Lett. **28**, 168 (1972); D. E. Aspnes, in *Proceedings of the 12th International Conference on the Physics of Semiconductors, Stuttgart, 1974,* Ref. 66, p. 1197; D. E. Aspnes and A. A. Studna, Surf. Sci. **96**, 294 (1980).
[83]M. R. Baklanov, K. K. Svitashev, L. V. Semenenko, and V. K. Sokolov, Opt. Spektrosk. **39**, 362 (1975) [Opt. Spectrosc. (USSR) **39**, 205 (1975)].
[84]Yu. B. Algazin, Yu. A. Blyumkina, N. I. Grebnev, K. K. Svitashev, L. V. Semenenko, and T. M. Yablontseva, Opt. Spektrosk. **45**, 330 (1978) [Opt. Spectr. (USSR) **45**, 183 (1978)].
[85]D. E. Aspnes and A. A. Studna, Rev. Sci. Instrum. **49**, 291 (1978).
[86]L. Viña and M. Cardona, Physica **117&118B**, 356 (1983).
[87]D. E. Aspnes and A. A. Studna, Phys. Rev. B **27**, 985 (1983).
[88]R. E. Lavilla and H. Mendlowitz, Appl. Opt. **6**, 61 (1967).
[89]G. E. Jellison, Jr., D. H. Lowndes, and R. F. Wood, Phys. Rev. B **28**, 3272 (1983).
[90]A. Compaan and H. J. Trodahl, Phys. Rev. B **29**, 793 (1984).
[91]F. Herman, R. L. Kortum, C. D. Kuglin, and J. P. van Dyke, in *Methods in Computational Physics,* edited by B. Alder, S. Fernbach, and M. Rotenberg (Academic, New York, 1968), Vol. 8, p. 193, and references therein.
[92]J. C. Phillips, Phys. Rev. **112**, 685 (1958); **125**, 1931 (1962); J. C. Phillips and K. C. Pandey, Phys. Rev. Lett. **30**, 787 (1973); K. C. Pandey and J. C. Phillips, Phys. Rev. B **9**, 1552 (1974).
[93]D. Brust, J. C. Phillips, and F. Basani, Phys. Rev. Lett. **9**, 94 (1962); F. Bassani and D. Brust, Phys. Rev. **131**, 1524 (1963); D. Brust, *ibid.* **134**, A1337 (1964); L. R. Saravia and D. Brust, *ibid.* **176**, 915 (1968); **178**, 1240 (1969).

[94]M. L. Cohen and T. K. Bergstresser, Phys. Rev. **141**, 789 (1966).
[95]M. Cardona and F. H. Pollak, Phys. Rev. **142**, 530 (1966).
[96]G. Dresselhaus and M. S. Dresselhaus, Phys. Rev. **160**, 649 (1967).
[97]C. W. Higginbotham, F. H. Pollak, and M. Cardona, Solid State Commun. **5**, 513 (1967).
[98]J. P. van Dyke, Phys. Rev. B **5**, 1489 (1972).
[99]W. D. Grobman, D. E. Eastman, and J. L. Freeouf, Phys. Rev. B **12**, 4405 (1975).
[100]J. R. Chelikowsky and M. L. Cohen, Phys. Rev. B **14**, 556 (1976).
[101]C. S. Wang and B. M. Klein, Phys. Rev. B **24**, 3393 (1981); **24**, 3417 (1981).
[102]M. L. Cohen and D. J. Chadi, in *Semiconductor Handbook,* edited by M. Balkanski (North-Holland, Amsterdam, 1980), Vol. 2, Chap. 4B.
[103]E. Antončik, Czech. J. Phys. **5**, 449 (1955).
[104]H. Y. Fan, Phys. Rev. **78**, 808 (1950); **82**, 900 (1951).
[105]M. L. Cohen, Phys. Rev. **128**, 131 (1962).
[106]P. Y. Yu and M. Cardona, Phys. Rev. B **2**, 3193 (1970).
[107]J. Camassel and D. Auvergne, Phys. Rev. B **12**, 3258 (1976).
[108]M. Schlüter, G. Martinez, and M. L. Cohen, Phys. Rev. B **12**, 650 (1975).
[109]P. B. Allen and V. Heine, J. Phys. C **9**, 2305 (1976); P. B. Allen, Phys. Rev. B **18**, 5217 (1978).
[110]P. B. Allen and M. Cardona, Phys. Rev. B **23**, 1495 (1981); **24**, 7479 (1981).
[111]P. B. Allen and M. Cardona, Phys. Rev. B **27**, 4760 (1983).
[112]H. Brooks, Adv. Electron. **7**, 85 (1955); V. Heine and J. A. Van Vechten, Phys. Rev. B **13**, 1622 (1976).
[113]G. E. Jellison, Jr., and F. A. Modine, J. Appl. Phys. **53**, 3745 (1982); Appl. Phys. Lett. **41**, 180 (1982); Phys. Rev. B **27**, 7466 (1983).
[114]J. C. Phillips, J. Phys. Chem. Solids **12**, 208 (1960).
[115]J. R. Chelikowsky and M. L. Cohen, Phys. Rev. Lett. **31**, 1582 (1973).
[116]M. Cardona, in *Modulation Spectroscopy,* edited by F. Seitz, D. Turnbull, and H. Ehrenreich (Academic, New York, 1966) [Solid State Phys. Suppl. **11**, 42 (1969)].
[117]Y. P. Varshni, Physica (Utrecht) **34**, 149 (1967).
[118]D. E. Aspnes, Appl. Phys. Lett. **39**, 316 (1981).
[119]D. E. Aspnes, Opt. Commun. **8**, 222 (1973); D. E. Aspnes and A. A. Studna, Appl. Opt. **14**, 220 (1975).
[120]Ablebond 36-2; Ablestik Laboratories 833 W. 182nd St., Gardena, Ca. 90248.
[121]The windows were made of Suprasil I, Heraeus Quartzschmelze, 6450 Hanau, Federal Republic of Germany.
[122]D. E. Aspnes, J. Opt. Soc. Am. **64**, 812 (1974).
[123]N. M. Bashara and R. M. Azzam, *Ellipsometry and Polarized Light* (North-Holland, Amsterdam, 1977).
[124]G. G. Devyatykh, E. M. Dianov, N. S. Karpychev, S. M. Mazavin, V. M. Mashinskiĭ, V. B. Neustruev, A. V. Nikolaĭchik, A. M. Prokhorov, A. I. Ritus, N. I. Sokolov, and A. S. Yushing, Kvant. Electron. (Moscow) **7**, 1563 (1980) [Sov. J. Quantum Electron. **10**, 900 (1981)].
[125]A. S. Householder, *Principles of Numerical Analysis* (McGraw-Hill, New York, 1953).
[126]A. Savitzky and J. E. Gollay, Anal. Chem. **36**, 1627 (1974); J. Steinier, Y. Termonia, and J. Deltour, *ibid.* **44**, 1906 (1972).
[127]D. E. Aspnes, Surf. Sci. **135**, 284 (1983).
[128]J. E. Rowe and D. E. Aspnes, Phys. Rev. Lett. **25**, 162 (1970).
[129]Y. Toyozawa, M. Inoue, T. Inui, M. Okazaki, and E. Hanamura, J. Phys. Soc. Jpn. Suppl. **21**, 133 (1967).
[130]C. D. Thurmond, J. Electrochem. Soc. **122**, 1133 (1975).
[131]D. E. Aspnes and J. E. Rowe, Phys. Rev. B **7**, 887 (1973).
[132]B. Velický and J. Sak, Phys. Status Solidi **16**, 147 (1966).
[133]E. O. Kane, Phys. Rev. **180**, 852 (1969).
[134]M. Cardona, in *Light Scattering in Solids II,* edited by M. Cardona and G. Güntherodt (Springer-Verlag, New York, 1982), p. 119.
[135]M. Cardona, Phys. Rev. B **15**, 5999 (1977).
[136]W. Hanke and L. J. Sham, Phys. Rev. B **21**, 4656 (1980); H. J. Mattausch, W. Hanke, and G. Strinati, *ibid.* **27**, 3735 (1983).
[137]A. Manoogian and A. Leclerc, Can J. Phys. **57**, 1766 (1979); Phys. Status Solidi B **92**, K23 (1979).
[138]L. Viña, C. Umbach, A. Compaan, M. Cardona, and A. Axmann, J. Phys. (Paris) Colloq. **44**, C5-203 (1983).
[139]L. Viña, H. Höchst, and M. Cardona (unpublished).